Optical and Acoustical Methods in Science and Technology

Influence of TDMAAs Acceptor Precursor on Performance Improvement of HgCdTe Photodiodes

P. Madejczyk[a], W. Gawron[a], A. Piotrowski[b], K. Kłos[b], J. Rutkowski[a] and A. Rogalski[a]

[a]Institute of Applied Physics, Military University of Technology, S. Kaliskiego 2, 00-908 Warsaw, Poland

[b]Vigo System S.A., Poznańska 129/133, 05-850 Ożarów Mazowiecki, Poland

One of the key factor which determine HgCdTe photodiode quality is acceptor doping efficiency. This paper presents significant progress made over the past three years in development of acceptor doping technology in metalorganic chemical vapour deposition HgCdTe photovoltaic detectors. High acceptor doping is required for P^+-contact layers, whereas low doping is necessary for p-type absorbing base layer. Previously, AsH_3 precursor was used as an acceptor dopant. This precursor is partially incorporated as electrically neutral As–H pairs, which are likely to be recombination centres in HgCdTe and in consequence influence on the carriers lifetime lowering. Substituting of AsH_3 by TDMAAs resulted in higher carrier lifetimes and thereby about one order of magnitude higher R_0A product of HgCdTe photodiodes in temperatures close to 230 K.

PACS numbers: 42.79.Pw, 07.57.Kp, 73.21.Cd, 78.67.Pt, 79.60.Jv

1. Introduction

The HgCdTe epilayers are the most significant material for high performance infrared detectors. The control of epilayer conductivity and doping level is still essential problem in the fabrication of HgCdTe infrared photodetectors [1]. MOCVD offers the possibility of realization the full flexibility of band-gap engineered HgCdTe heterostructures with acceptor and donor dopant sources enable the control of carrier concentrations over the wide required ranges.

The Auger lifetime in HgCdTe is a key parameter in determining the upper limit of detector performance such as quantum efficiency, dark current and noise. Hence the Auger lifetime value plays a crucial role in determining the choice of material type used as the active region of an IR detector.

Figure 1 presents example of the structure of HgCdTe photodiode. Symbol "+" denotes high level doping, capital letter — wider gap. Improving the quality of p-type layers shown in the structure (Fig. 1) constitutes the main subject of this paper. Control of the donor doping seems to be well established, while the acceptor doping controlling is more difficult and requires careful studies. High acceptor doping is required for P^+-contact layers, whereas low doping is necessary for absorbing p-type base layer.

At the beginning AsH_3 has been used as acceptor precursor. Mitra et al. [2] suggested that As doping of CdTe with AsH_3, causes the incorporation of As–H pairs in addition to As. These As–H complexes are expected to be electrically neutral but they are likely to be recombination centers in HgCdTe. As a result, p-type arsenic doped HgCdTe epilayers using AsH_3 should be characterized by carrier lifetimes lower than that doped with Trisdimethylaminoarsenic (arsenic presursor), (TDMAAs). Following this suggestion we installed TDMAAs line and alternatively used mentioned two precursors. This paper presents influence of acceptor doping technology improvement on HgCdTe photodiode parameters.

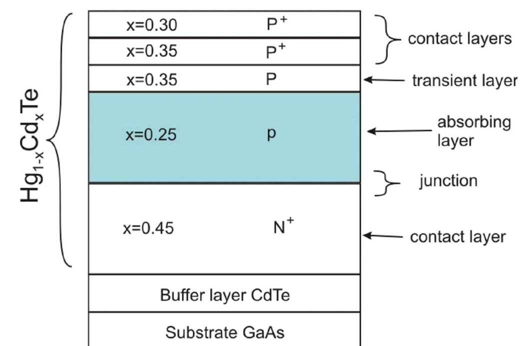

Fig. 1. Example of the structure of HgCdTe photodiode.

2. Growth and characterization of HgCdTe structures

The HgCdTe layers were grown in a horizontal, near atmospheric pressure MOCVD reactor with H_2 carrier gas, using the following precursors: di-isopropyl telluride (DiPTe), di-methyl cadmium (DMCd) and ele-

mental mercury. The As doping was achieved using one of two arsenic precursors installed in our system: AsH_3 or TDMAAs. The special partition in the reactor separates As precursors from DMCd to prevent premature reaction. Growth was carried out at temperature about 350 ℃ onto GaAs substrates orientated 3° off (100) towards the nearest (110) using the interdiffused multilayer process (IMP) technique. Tellurium flush during nucleation process provides (111)CdTe growth. Typically 3–4 μm thick CdTe layer was used as a buffer layer reducing stress caused by crystal lattice misfit between GaAs and HgCdTe. Depending on the heterostructure thickness, the (111)HgCdTe layers with surface roughness from 50 nm to 120 nm have been obtained. Surface roughness parameter Rq was estimated using Wyko 1100 profiler. Detailed study of HgCdTe surface morphology has been described earlier [3].

The thickness of the HgCdTe layers was determined from the cleavage profile. The $Hg_{1-x}Cd_xTe$ epilayer composition was estimated analyzing Fourier transform infrared (FTIR) spectrum of the layer. More comprehensive details of the growth experiments performed in our laboratory were published elsewhere [4].

The carrier concentration was determined using 77 K fixed field Van der Pauw–Hall measurements at a magnetic field of 0.175 T in close dewar configuration. The temperature dependent photoconductance-lifetime was measured at 1550 nm InGaAsP modulated laser diode driven by pulsed generator. This excitation system had a fall time of about 40 ns.

Figure 2 presents residual background concentration of undoped HgCdTe layers versus consecutive number of growth processes carried out within the last three years. The included data are from the period since August 2006 (when we started using TDMAAs) up to the time of writing this report. At the beginning, high residual both donor and acceptor concentrations indicated strong contamination. The precise Hall measurements at liquid nitrogen temperature pointed the GaAs substrates as the reason of impurities $> 10^{16}$ cm^{-3} caused by Cu contamination. The negotiation with GaAs substrates supplier and their modified substrate preparation method resulted in reduction of residual background concentration to the level of (1–3) $\times$ 10^{15} cm^{-3}. The increase of the background concentration between #1700 and #1900 processes resulted most probably from the leak in our metal-organic chemical vapor deposition (MOCVD) system. The reason of increase of the residual concentration is mostly uncertain. The best results reported from other labs disclose the residual donor concentration at the level of mid 10^{14} cm^{-3} so the fight with impurities goes on in our lab. The matter of residual donor concentration is particularly important during *p*-type doping at the low level.

Figure 3 presents incorporation and activation of As from TDMAAs and AsH_3 versus precursor partial pressure. Incorporation of arsenic was determined by secondary ion mass spectroscopy (SIMS) measurements.

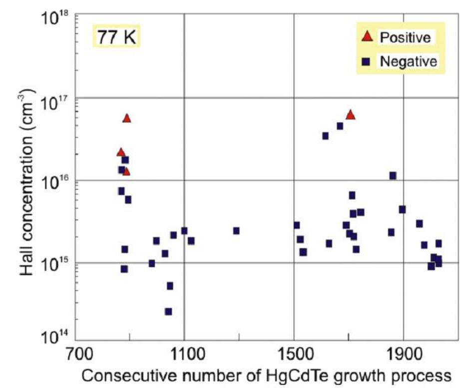

Fig. 2. Residual background concentrations of undoped HgCdTe layers versus the numbers of growth processes.

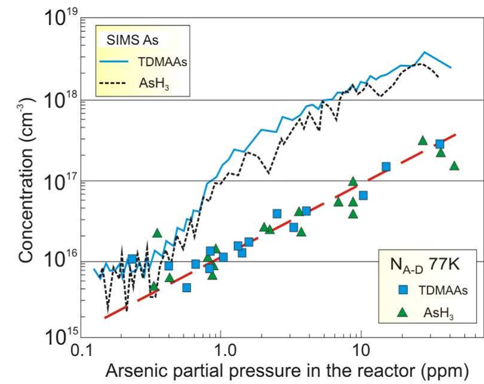

Fig. 3. Incorporation and activation of As from TDMAAs and AsH_3 versus partial pressure of precursors.

The levels of As incorporation from AsH_3 and TDMAAs into growing HgCdTe samples are equal considering the measurement uncertainty. The As chemical concentration increases roughly proportionally with As precursor partial pressure up to 10 ppm. Higher level of As precursor injection does not result in proportional As-incorporation due to the saturation effect. Arsenic precursors were introduced to the reactor during CdTe cycles of IMP growth process. Introducing of AsH_3 or TDMAAs during both CdTe and HgTe does not result in the increase of incorporation. It is worth to note that introducing As precursor into reactor accelerates DMCd pyrolysis that causes considerable shift in x composition. For example, 20 ppm dose of TDMAAs increases x composition from planned 0.3 to 0.4. Figure 4 shows that chemical concentration determined by SIMS does not agree with acceptor electrical concentration determined by 77 K Hall measurements of HgCdTe epilayers grown in our laboratory. For mid and high levels of acceptor doping, the gap between chemical and electrical concentration is about an order of magnitude. So, we do not observe 100% of arsenic activation unlike reported by other authors [5]. Post growth annealing in temperatures $\approx$ 400 ℃ did not bring arsenic activation increasing.

For full heterostructure doping technology development it is essential to provide careful study of single layer doping analysis. Figure 4 presents the Hall concentration versus reciprocal temperature for $Hg_{0.73}Cd_{0.27}Te$ layer doped with 0.3 ppm TDMAAs. At the beginning, the Van der Pauw sample of as-grown layer was cut, fixed in four probe handle and measured in the constant magnetic field as a function of temperature. This measurement results are represented by points creating the upper curve. Next the sample was chemically etched in 5% bromo-glycol solution in order to remove surface skin layer about 0.5 μm thick. The Hall measurements of etched sample were repeated and the results are represented by points arranging the lower curve. The difference between these two measurements is about an order of magnitude in the Hall concentration. Such phenomenon is well known and described in the literature [6]. Surface n-type layer on p-HgCdTe sample is caused by native oxide ($\approx 10^{12}$ cm^{-2}) which influence on difficulties in the Hall data interpretation. Surface passivation does not always bring desirable results due to n-type inversion layer. One of quantitative technique which can help interpret p-HgCdTe Hall data is quantitative mobility spectrum analysis (QMSA) [7]. Using this technique, both free-carrier densities and mobilities can be automatically determine from magnetic field dependent Hall and resistivity data. However, for unambiguous interpretation of experimental results, the required μB (mobility $\times$ magnetic field) product should be $> 10^8$ cm^2 G/(V s), which is difficult to fulfil for HgCdTe heavy holes even at the highest magnetic field values. An alternative analysis is the two-layer model developed by Wong [8], which can utilize much smaller magnetic fields and is ideal for p-type HgCdTe with possible n-type interfaces. In p-HgCdTe sample Hall measurements electrical contacts quality plays key role. Rockwell used front-surface, wire-bonded contacts [9], whereas soldered In contacts were used at West Virginia University [10]. In our laboratory, we elaborated different methods which ensure high repeatability and low measure deviation for the set of samples coming from one growth process. The four corners of square Van der Pauw sample are scratched by steel needle. This solution removes passivation layer and possible surface oxides and provides larger surface for golden contact coating deposited from water solution of $AuCl_3$. Indium balls are put and lightly pressed on dry golden corners. Such procedure eliminates most anomalous effect observed during p-type HgCdTe electrical measurements.

Figure 5 shows the 77 K Hall concentration estimated from SIMS profile of HgCdTe sample doped with 17 ppm of AsH_3 for (111) and (100) crystallographic orientations. We can observe that arsenic chemical concentration determined by SIMS is an order of magnitude grater for (100) orientation than for (111) orientation. Explanation of this difference by surface structure analysis was expounded by Svob et al. [11]. In spite of better arsenic incorporation for (100)HgCdTe, our studies

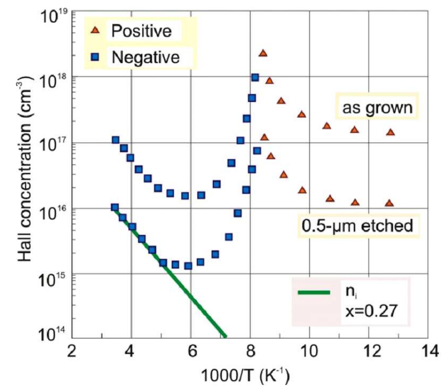

Fig. 4. Hall concentration versus reciprocal temperature of $Hg_{0.73}Cd_{0.27}Te$ doped with 0.3 ppm TDMAAs.

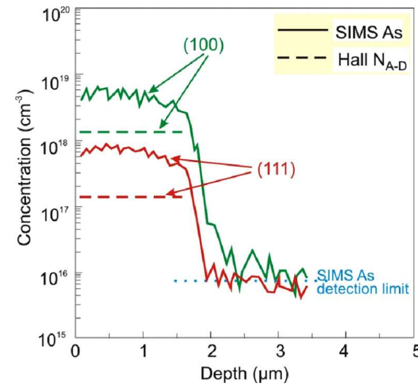

Fig. 5. Hall data estimated with SIMS profile of HgCdTe sample doped with 17 ppm of AsH_3 for (111) and (100) crystallographic orientations.

on this layer crystallographic orientation were suspended due to lack of the progress in morphology improvement. The (100)HgCdTe layers were covered by high density of hillocks of height comparable with layer thickness which disqualified them for devices fabrication. Holes concentrations determined by the Hall measurements are almost an order of magnitude lower than chemical concentration, which suggests medium activation of arsenic. In order to check the possibility of arsenic activation increase, the selected samples were annealed in two zone furnace in temperatures close to 400 °C in mercury vapours presence. One of result of such annealing is presented in Fig. 6. It is clearly seen that the Hall concentration as well as the Hall mobility did not change significantly after annealing. The lack of changes in the Hall concentration after annealing can also suggest that the level of possible mercury vacancies is below intentional arsenic doping level. Annealing in temperatures higher than 430 °C even during short times (few minutes) destroys the sharpness of interfaces.

Figure 6 shows comparison of measured lifetimes for p-type mid-wavelength infrared (MWIR) and long-wavelength infrared (LWIR) HgCdTe doped with AsH_3

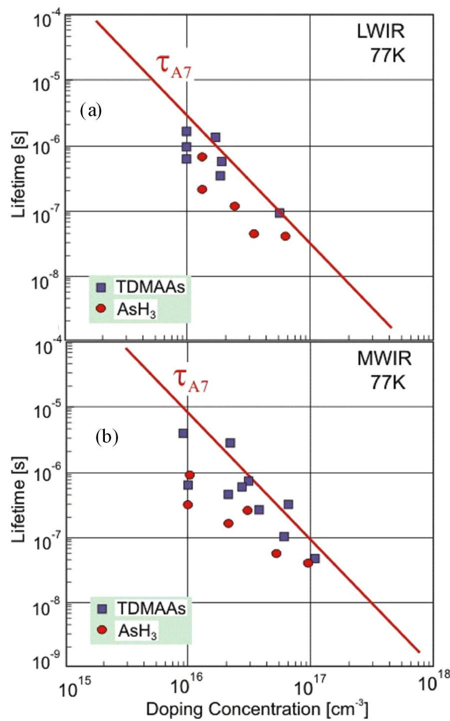

Fig. 6. Measured lifetimes for p-type LWIR (a) and MWIR (b) HgCdTe epilayers at 77 K compared to theoretical Auger 7 lines.

or TDMAAs. Measurements were conducted at 77 K using photoconductive decay technique. The presented results show that carrier lifetimes for p-HgCdTe doped with AsH_3 or TDMAAs are comparable within the range of measurement uncertainty and are limited by Auger 7 process. Solid lines for both LWIR and MWIR HgCdTe samples denote Auger 7 theoretical lines based on the Krishnamurthy et al. calculations [12]. Their model use algorithms for computing 8-fold integral representing the Auger rate and use a detailed band structure based on long range Hamiltonian in the tight binding form. These calculations were partially confirmed by experimental results summarized by Kinch et al. [13]. About 70% of samples (within the range of measurement uncertainty) manifest similar values as presented in Fig. 7. The other 30% of samples population present quite different values. Due to the Shockley-Hall-Read (SHR) centers, the measured carrier lifetimes may differ even one or two orders of magnitude from expected Auger 7 values.

Table summarizes selected data for p-type (111)HgCdTe TDMAAs doped samples for different composition x-values. The gathered values of carrier lifetimes in this table and in Fig. 6 excess the values presented by Lopes et al. [14] about one order of magnitude and confirm the new model proposed by Krisnamurthy et al. [15]. Doping profile study and understanding the electrical properties of single layers enable to control compound HgCdTe heterostructure deposition for infrared photodiode fabrication.

TABLE

Data of selected p-type (111) $Hg_{1-x}Cd_xTe$ samples doped with TDMAAs.

x	TDMAAs [ppm]	II/VI ratio	SIMS [cm^{-3}]	Rsqr* [Ω/]	n_H^* [cm^{-3}]	μ_H^* [cm^2/V s]	τ^* [ns]
0.237	0.8	1.5	4.6×10^{16}	649	2.4×10^{16}	400	240
0.26	0.8	1.5	2.9×10^{16}	860	1.3×10^{16}	211	1460
0.24	18	3.0	5.7×10^{17}	249	2.3×10^{17}	300	> 40
0.27	0.17	1.5	3.21×10^{16}	939	1.38×10^{16}	484	880
0.28	5	3.0	4.4×10^{17}	1001	1.6×10^{17}	428	660
0.37	18	3.0	7.1×10^{17}	4800	2.1×10^{17}	300	2000
0.32	10	5	5.0×10^{17}	6804	2.2×10^{17}	204	6500
0.50	25	5.4	–	1152	2.7×10^{17}	50	7400
0.50**	25	5.4	–	1082	1.76×10^{17}	37	–

* measured at 77 K; ** TDMAAs dose in both CdTe and HgTe cycles of IMP growth

Figure 7 presents SIMS profile of typical MWIR photodiode structure doped with TDMAAs and ethyliodide (EI). The valuable information provided by SIMS concerns levels of chemical concentrations of both acceptor and donor dopants. TDMAAs dose of 28 ppm provide As chemical concentration at the level of 1×10^{18} cm^{-3} which is sufficient for p-type contact layer deposition. About 7 ppm of EI is sufficient for N^+-contact layer fabrication. From point of view of photodiode design, particularly important is the sharpness of the interfaces. The sharp-

ness of As interfaces is about one order of magnitude per 0.5 μm, which is in the range of acceptance. The iodine remains in p-type absorbing layer and is a matter of some concern. The iodine tail may be caused by diffusion during growth or by memory effect.

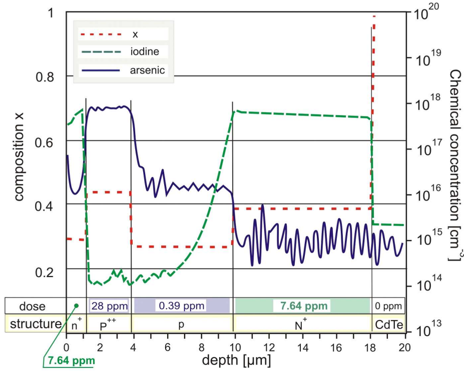

Fig. 7. SIMS profile of typical MWIR photodiode structure doped with TDMAAs and EI.

3. R_0A product

Detectivity of infrared photodiode can be determined by the following Eq. [16, 17]:

$$D^* = \frac{R_v A^{1/2}(\Delta f)^{1/2}}{V_n} = \frac{\eta\lambda q}{hc}\left(\frac{4kT}{R_0A} + 2q^2\eta\Phi_{\rm b}\right)^{-1/2}, \qquad (1)$$

where η is the quantum efficiency, q is the electron charge, and $\Phi_{\rm B}$ is the background flux density.

For the last formula we may distinguish two important cases:

- background-limited performance; if $4kT/R_0A \ll 2q^2\eta\Phi_{\rm B}$, then we obtain

$$D^*_{\rm BLIP} = \frac{\lambda}{hc}\left(\frac{\eta}{2\Phi_{\rm B}}\right)^{1/2}, \qquad (2)$$

- thermal noise limited performance; if $4kT/R_0A \gg 2q^2\eta\Phi_{\rm b}$, then

$$D^* = \frac{\eta\lambda q}{2hc}\left(\frac{R_0A}{kT}\right)^{1/2}. \qquad (3)$$

The last equation indicates that the R_0A product determines directly the most important parameter of IR detector — detectivity.

For an n-on-p diode structure, the junction resistance is limited by diffusion of minority carriers from the p-side into the depletion region. In the case of conventional bulk diodes, where thickness of active region $t \gg L_{\rm e}$ ($L_{\rm e}$ is the minority diffusion length), the R_0A product is equal to

$$(R_0A)_{\rm D} = \frac{kT}{qJ_{\rm s}}\frac{(kT)^{1/2}}{q^{3/2}n_{\rm i}^2}N_a\left(\frac{\tau_{\rm e}}{\mu_{\rm e}}\right)^{1/2}, \qquad (4)$$

where $J_{\rm s}$ is the current density, $n_{\rm i}$ is the intrinsic carrier concentration, N_a is the doping concentration, and $\mu_{\rm e}$ and $\tau_{\rm e}$ are the minority carrier mobility and lifetime. The R_0A product (saturation current density) is proportional (inversely proportional) to $N_a\tau_{\rm e}^{1/2}$. By thinning the substrate to a thickness smaller than the minority-carrier diffusion length (thus reducing the volume in which diffusion current is generated) the corresponding dark current decreases, provided that the back surface is properly passivated to reduce surface recombination. As a result, the current density can decrease by a factor of $L_{\rm e}/t$. If the thickness of the p-type region is such that $t \ll L_{\rm e}$, we obtain

$$(R_0A)_{\rm D} = \frac{kT}{q^2}\frac{N_a}{n_{\rm i}^2}\frac{\tau_{\rm e}}{t}. \qquad (5)$$

On the contrary, if $t \ll L$, the R_0A product (saturation dark current) is proportional (inversely proportional) to $N\tau u$ Of course, analogical formulae can be obtained for p-on-n junctions.

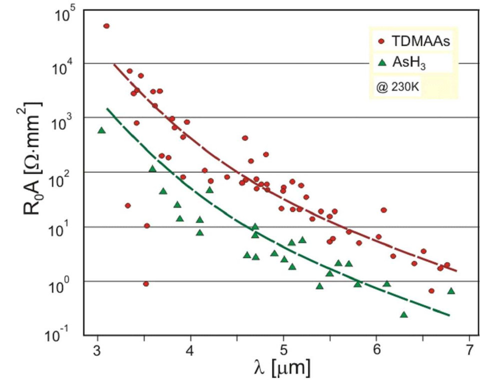

Fig. 8. R_0A product at 230 K as a function of cut--off wavelength for MWIR photodiodes with absorbing layers doped with AsH_3 and TDMAAs.

Both Eqs. (4) and (5) indicate that increase of minority carrier lifetime causes increase of the R_0A product.

Figure 8 shows R_0A product of MWIR HgCdTe photodiodes with absorbing layers doped with AsH_3 and TDMAAs measured at 230 K as a function of cut-off wavelength. As we can see, the R_0A product is about one order of magnitude higher for structures doped with TDMAAs than those doped with AsH_3 in the wavelength range from 3 μm to 7 μm. This is confirmation of presumption suggested by Mitra et al. [2] about unfavourable incorporation of As–H pairs from AsH_3 into growing HgCdTe epilayers. Increase of the R_0A product is consequence of increasing minority carrier lifetime due to using TDMAAs precursor. This is also partially result of the progress in device fabrication in our laboratory, especially IMP growth modification, residual background concentration reduction, and surface morphology improvement.

4. Conclusions

In the paper influence of acceptor doping technology improvement on MWIR HgCdTe photodiode parameters

is shown. The TDMAAs and AsH_3 were compared as an effective p-type doping precursors. Over a wide range of $Hg_{1-x}Cd_xTe$ compositions ($0.17 < x < 0.4$) the acceptor doping concentrations in the range from 5×10^{15} cm^{-3} to 5×10^{17} cm^{-3} were obtained without post growth annealing. It was shown that incorporation and arsenic activation depends strongly on HgCdTe layer crystallographic orientation. The lifetime measurements indicate that Auger 7 mechanism has decisive influence on carrier lifetime in p-type HgCdTe epilayers. Substituting of AsH_3 by TDMAAs contributed also to increase the safety level in our laboratory.

This paper presents also significant progress made over the past three years in development of acceptor doping MOCVD HgCdTe photodiode fabrication. High acceptor doping is required for P^+-contact layers, whereas low doping is necessary for p-type absorbing base layers. Increase of the R_0A product of MWIR HgCdTe photodiodes is a consequence of increasing minority carrier lifetime due to using TDMAAs precursor, IMP growth modification, residual background concentration reduction, and surface morphology improvement.

Acknowledgments

This work was partially supported by the Polish Ministry of Science and Higher Education as research projects No. PBZ MNiSW 02/I/2007 and European project No. POIG.01.03.01-14-01/08.

References

[1] A. Rogalski, *Rep. Prog. Phys.* **68**, 2267 (2005).

[2] P. Mitra, F.C. Case, M.B. Reine, *J. Electron. Mater.* **27**, 510 (1998).

[3] P. Madejczyk, A. Piotrowski, K. Kłos, W. Gawron, A. Rogalski, J. Rutkowski, W. Mróz, *Bull. Pol. Acad. Sci.: Tech. Sci.* **57**, 173 (2009).

[4] P. Madejczyk, A. Piotrowski, W. Gawron, K. Kłos, J. Pawluczyk, J. Rutkowski, J. Piotrowski, A. Rogalski, *Opto-Electron. Rev.* **13**, 239 (2005).

[5] C.D. Maxey, I.G. Gale, J.B. Clegg, P.A.C. Whiffin, *Semicond. Sci. Technol.* **8**, S183 (1993).

[6] M.A. Kinch, *Fundamentals of Infrared Detector Materials*, SPIE Press, Bellingham 2007.

[7] G.K.O. Tsen, C.A. Musca, J.M. Dell, J. Antoszewski, L. Faraone, *J. Electron. Mater.* **36**, 826 (2007).

[8] T. Wong, M.Sc. Thesis, Massachusetts Institute of Technology, 1974.

[9] E.C. Piquette, DD. Edwall, D.L. Lee, J.M. Arias, *J. Electron. Mater.* **35**, 1346 (2006).

[10] C.H. Swartz, R.P. Tompkins, N.C. Giles, T.H. Myers, D.D. Edwall, J. Ellsworth, E. Piquette, J. Arias, M. Berding, S. Krishnamurthy, I. Vurgaftman, J.R. Meyer, *J. Electron. Mater.* **33**, 728 (2004).

[11] L. Svob, I. Cheye, A. Lusson, D. Ballutaud, J.F. Rommeluere, Y. Marfaing, *J. Cryst. Growth* **184/185**, 459 (1998).

[12] S. Krishnamurthy, T.N. Casselman, *J. Electron. Mater.* **29**, 828 (2000).

[13] M.A. Kinch, F. Aqariden, D. Chandra, P–K Liao, H.F. Schaake, H.D. Shih, *J. Electron. Mater.* **34**, 880 (2005).

[14] V.C. Lopes, A.J. Syllaios, M.C. Chen, *Semicond. Sci. Technol.* **8**, 824 (1993).

[15] S. Krishnamurthy, M.A. Berding, Z.G. Yu, C.H. Swartz, T.H. Myers, D.D. Edwall, R. DeWames, *J. Electron. Mater.* **34**, 873 (2005).

[16] A. Rogalski, *Acta Phys. Pol. A* **116**, 389 (2009).

[17] A. Rogalski, K. Adamiec, J. Rutkowski, *Narrow-Gap Semiconductor Photodiodes*, SPIE Press, Bellingham 2000.